2016

Novel Airside Heat Transfer Surface Designs Using an Integrated Multi-Scale Analysis with Topology and Shape Optimization

Daniel Bacellar
University of Maryland, United States of America, dfbace@umd.edu

Vikrant Aute
University of Maryland, United States of America, vikrant@umd.edu

Zhiwei Huang
University of Maryland, United States of America, zwhuang@umd.edu

Reinhard Radermacher
University of Maryland, United States of America, raderm@umd.edu

Novel Airside Heat Transfer Surface Designs Using an Integrated Multi-Scale Analysis with Topology and Shape Optimization

Daniel BACELLAR[1], Vikrant AUTE[2]*, Zhiwei, HUANG[3], Reinhard RADERMACHER[4]

[1,2,3,4]Center for Environmental Energy Engineering
Department of Mechanical Engineering, University of Maryland
College Park, MD 20742 USA
[1]Tel: 301-405-7314, [2]Tel: 301-405-8726, [3]Tel: 301-642-2131, [4]Tel: 301-405-5286
Email: [1]dfbace@umd.edu, [2]vikrant@umd.edu, [3]zwhuang@umd.edu, [4]raderm@umd.edu

* Corresponding Author

ABSTRACT

The major limitation of air-to-refrigerant Heat eXchangers (HX) is the airside thermal resistance which can account for more than 90% of the overall thermal resistance. The current research on heat transfer augmentation extensively focuses on the secondary heat transfer surfaces (fins). The main reason is that the heat transfer coefficient on the primary surfaces (tubes) is usually not sufficiently high to provide a minimum thermal resistance without significantly increasing the HX size. One contributing factor is the tube size; the reduction of the hydraulic diameter significantly improves performance and compactness. Another contributing factor is the shape of the tube itself, which is generally limited to circular, oval, or flat. In this paper, we investigate three novel surface concepts, using NURBS and ellipse arcs, focusing on the airside tube shape with small flow channels aiming at the minimization or total elimination of fins. The study constitutes designing a 1.0kW air-to-water HX, using an integrated multi-scale analysis with topology and shape optimization methodology. We leverage automated CFD simulations and Approximation Assisted Optimization (AAO), thus, significantly reducing the computational time and resources required for the overall analysis. The resulting optimum designs exhibit capacity similar to a baseline microchannel HX (MCHX), with same flow rates and 10% reduced approach temperature, more than 20% reduction in pumping power, more than 20% reduction in size. Experimental validation for a proof-of-concept design is conducted and the predicted heat capacity agrees within 5% of the measured values, whereas the airside pressure drop agrees within 10%.

1. INTRODUCTION

The research on heat transfer augmentation (HTA) relentlessly seeks to develop highly compact heat exchangers (CHX) with high performance surfaces. A CHX is the definition of high surface-to-volume ratio (Kays & London, 1984). According to Shah and Sekulic (2003) a CHX has a surface-to-volume ratio of least 7.0cm²/cm³, or a hydraulic diameter smaller than 6.0mm. Amongst the various HTA techniques, the passive methods (no external power required) (Webb & Kim, 2005) are the most used in air-to-refrigerant HX applications, and thus the focus of this paper.

Enhanced secondary heat transfer surfaces (fins) are an effective way to achieve compact high-performance surfaces. External fins enhancement is widely studied and a great variety of designs and concepts for augmentation of heat transfer are available in the literature (DeJong & Jacobi, 2003; Gholami et al., 2014). While such approach may be effective, it also entails a few penalties, including: a) increased viscous dissipation, thus increasing pressure drop; b) higher manufacturing and material costs; c) intensification of fouling, and/or frosting (evaporator applications) and thus degrading the thermal-hydraulic performance.

Another way of achieving significant heat transfer enhancement is by reducing the tube size. Small diameter tubes yield high transfer enhancement due to their high surface area to volume ratio, significant material reduction, and refrigerant side volume reduction; but most importantly due to significant enhancement in heat transfer coefficient (Bacellar et al., 2014; Kasagi et al., 2003; Paitoonsurikarn et al., 2000; Bacellar et al., 2015).

One major limitation regarding primary heat transfer surface is the tube geometry itself, which is typically limited to round, elliptical or flat shapes. Although elliptical (Min & Webb, 2004; Matos et al., 2004) and flat tubes (Joardar &

Jacobi, 2005) have lower friction loss compared to round tubes, they do not necessarily yield a better thermal-hydraulic performance. There is yet, much more to improve with respect to tube shapes. More recently, Hilbert et al. (2006) and Ranut et al. (2014) introduced tube shape optimization for lower Reynolds numbers on the airside using NURBS. Both studies focused specifically on the effects of the tube shape on the fluid flow, without accounting for scaling and topology variables. Although their analyses are not extensible to full-scale HX applications, they pioneered on performing a general shape optimization of primary heat transfer surfaces for a tube bundle in cross flow configuration.

This paper presents the application of an integrated multi-scale analysis and shape optimization method for CHX design (Bacellar et al., 2016) to three novel airside surfaces with tube ranging from 0.5mm to 2.0mm in height. Comprehensive numerical verification and experimental validations are carried out.

2. METHODOLOGY

2.1 Design and optimization framework

The numerical optimization framework (Figure 1) consists of an Approximation Assisted Optimization (Abdelaziz et al., 2010), which involves four main steps: a) Problem specification and Design of Experiments (DoE) development; b) CFD modeling and Simulations; c) Metamodel development; d) Multi-Objective Optimization.

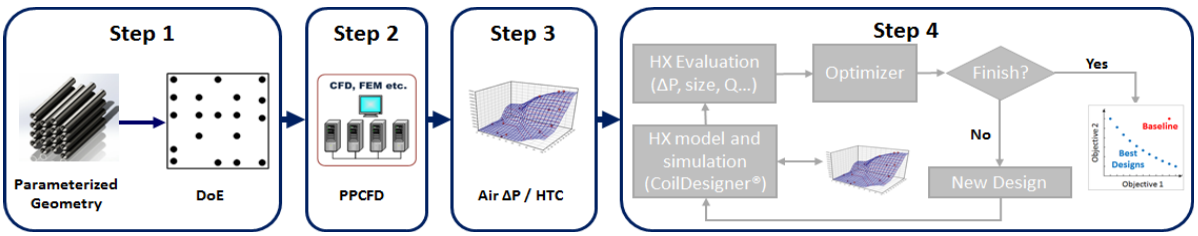

Figure 1: Optimization framework.

2.2 Problem Specification

In this paper, we investigate an air-to-water HX in cross-flow configuration. The major assumptions for the HX models include: a) air velocity uniformly distributed and normal to the face area; b) uniform distribution and fully developed flow on the waterside. Computational Fluid Dynamics (CFD) simulations carried out to evaluate the airside thermal-hydraulic performance. The waterside Reynolds numbers (based on the cross section hydraulic diameter) are much lower than 1000, which lead to a reasonable preliminary assumption of laminar flow, therefore the use of existing correlations for small flow channels in single phase is valid.

We investigated three novel surfaces (see Figure 2) namely: a) Finless NURBS tube HX (NTHX); b) Webbed NURBS tube HX (WTHX); c) Airfoil HX (AFHX). The first is a finless tube bundle in staggered arrangement with NURBS shaped tubes. The second (Figure 3) consists of a multi-port web with NURBS shaped channels. Unlike the NTHX, the WTHX channels are arranged in an in-line fashion. The third is a multiport airfoil shaped tube arranged in such way that the air passage is constant between tubes, inspired by the rotating fins concept from Koplow (2010).
The DoE for each surface contains 1600 designs for both NTHX and WTHX, and 500 designs for AFHX. The number of designs varies according to the number of design variables, which for the NTHX and WTHX is 14, while the AFHX has only 5. The DoE is generated using an augmented Latin Hypercube Sampling.

Finally, the objective is to design a novel HX that can outperform a state-of-the-art HX while occupying a smaller envelope volume. The selected baseline is a 1.0kW air-to-water microchannel HX (MCHX).

2.3 CFD Modeling

The CFD computational domain (Figure 4) is a two dimensional cross section segment of the HX, assuming any end effects to be negligible. The inlet boundary has uniform velocity and uniform temperature (300K), whereas the outlet boundary is at constant atmospheric pressure. The upper and lower boundaries are periodic, and the tube walls are at constant temperature of 340K. The fluid properties use ideal gas model, and the turbulence is evaluated using the k-kl-ω transition model. The convergence criteria used is 10^{-5}. The near wall region mesh is a fine map scheme with growing layers at a ratio of 1.2. The core of the computational domain is a pave mesh scheme with an average element size equal to the last row of the boundary layer mesh.

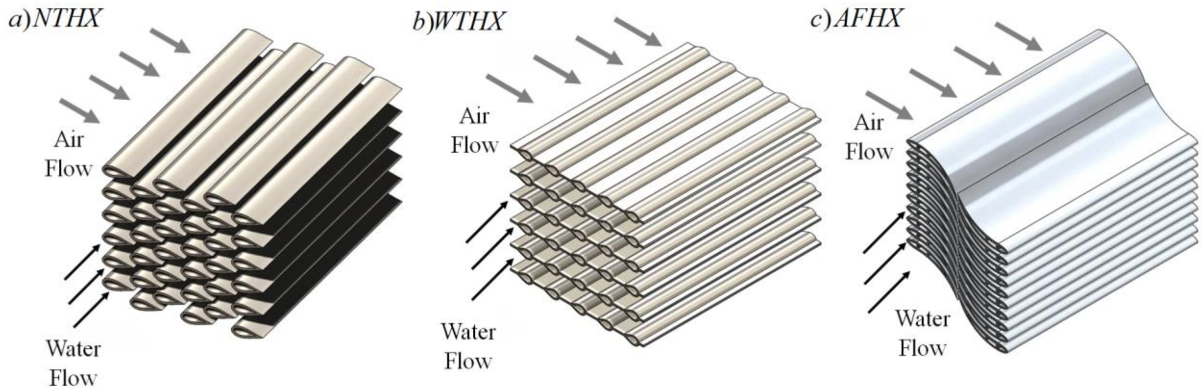

Figure 2: HX Concepts: a) NTHX; b) WTHX; c) AFHX.

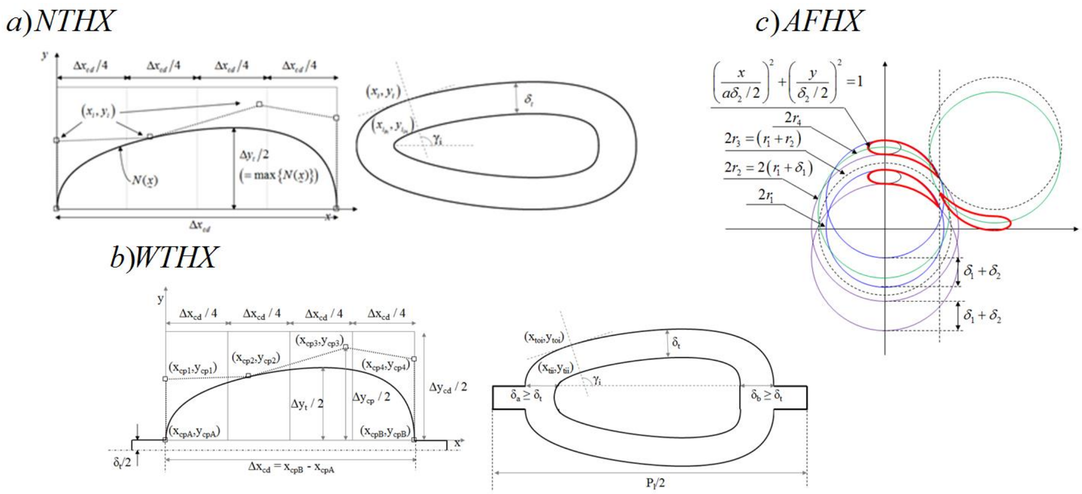

Figure 3: Tube shape parameterization: a) NTHX; b) WTHX; c) AFHX.

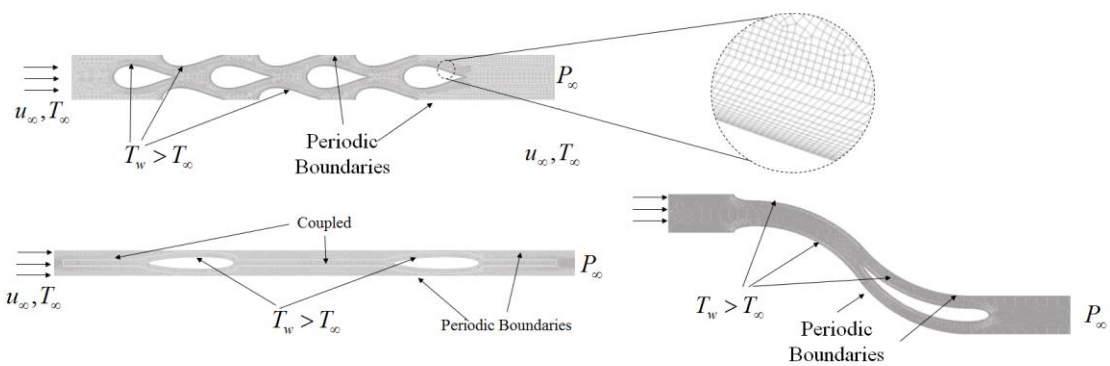

Figure 4: CFD Computational domains.

2.3.1 CFD data reduction

Since the CFD models serve to determine the airside thermal and hydraulic resistances, there is no need to account for additional thermal resistances. Thus with constant wall temperature, the capacitance ratio yields C_{min} / C_{max} = 0, then the heat transfer coefficient can be easily calculated through ε-NTU method as per equations (1-2). The pressure drop is determined as the difference between inlet and outlet static pressures, assuming that acceleration pressure drop and local losses are negligible.

$$NTU = -\ln\left(1-\varepsilon\right) = -\ln\left[1-\left(T_{out}-T_{in}\right)/\left(T_{wall}-T_{in}\right)\right] \tag{1}$$

$$h = UA/A_o = NTU \cdot C_{\min}/A_o \tag{2}$$

2.3.2 Parallel Parameterized CFD

Simulating the entire DoE in CFD is a computationally expensive task, particularly for complex problems, and it can be infeasible if one approaches it manually. The Parallel Parameterized CFD (PPCFD) (Abdelaziz et al., 2010) is a methodology that automates the CFD simulations. The code developed consists modules for reading and writing input/output data from DoE to journal files and from CFD output to post-processed data. The interaction between the code and the CFD environment occurs internally and in an automated fashion without user interaction.

2.3.3 CFD Uncertainty Analysis

A common way of determining the CFD model uncertainty is the Grid Convergence Index (GCI) (equation 3) method (Roy & Oberkampf, 2011; ASME, 2009; Roach, 1997), which quantifies the uncertainty associated to the grid resolution for at least three sizes. Bacellar et al. (Bacellar et al., 2014) have demonstrated that the designs at the boundary of the design space have higher uncertainties than that of any design within the design space; since the combinations of lower and upper bounds yield the most awkward shaped computational domains they potentially result in poorer grids. In this study the investigation comprised of quantifying the uncertainty of the boundary designs for three grid resolutions and at a constant refinement ratio ($r_{21} = r_{32} = r = 1.3$). According to Roach (1997) the factor of safety (F_s) recommended is 3.0. Additionally the observed order of accuracy (p) is limited to a lower bound of 0.5 and an upper bound of 2.0, which is the expected order of accuracy. This bounding avoids unreasonable uncertainty estimations (Roy & Oberkampf, 2011). Figure 5 and Figure 6 present the summarized results for this analysis.

$$GCI_{\phi} = F_s \cdot e_{\phi}^{21} \Big/ \left(r^{p\left(e_{\phi}^{21}, e_{\phi}^{32}\right)} - 1 \right) \tag{3}$$

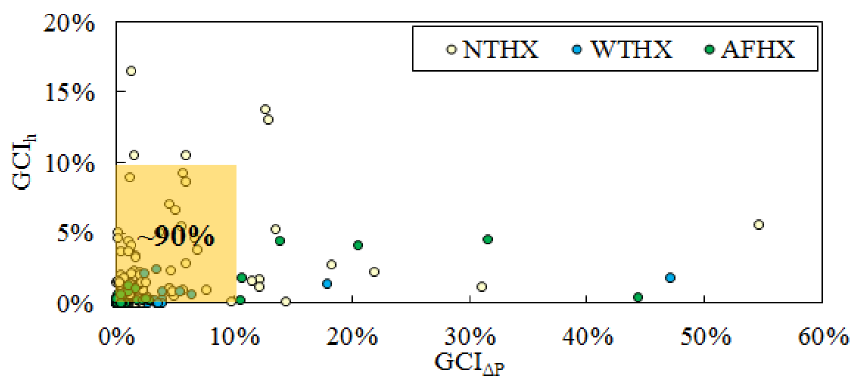

Figure 5: CFD Uncertainty Analysis.

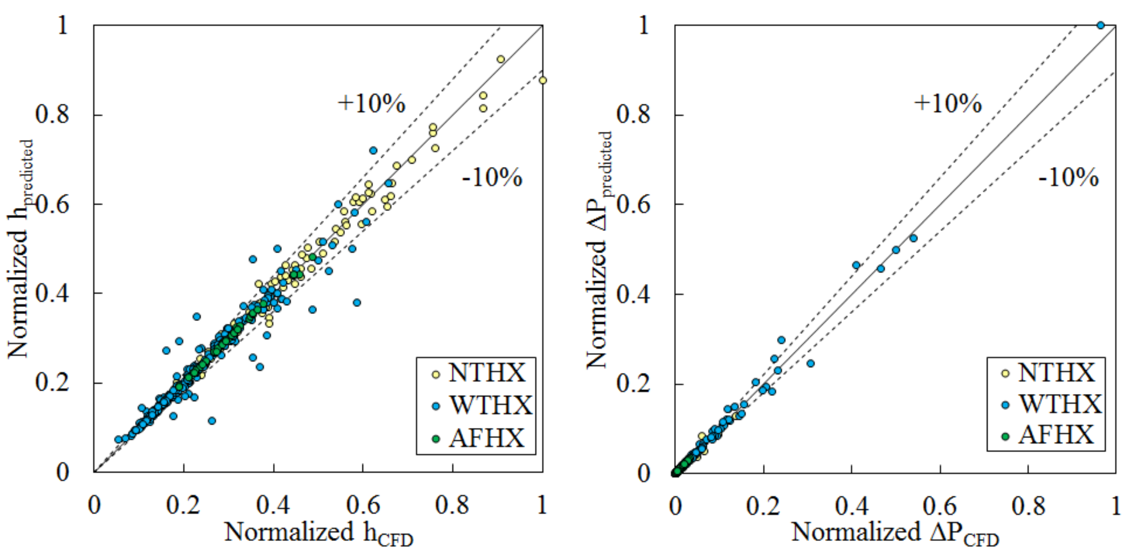

Figure 6: Metamodel Verification Results.

2.4 CFD Metamodels

The metamodel verification comprises evaluating its ability of predicting responses for randomly chosen designs and comparing them to actual CFD simulations. In this study, the metamodel "goodness" is evaluated using the Metamodel Acceptability Score (MAS) (Hamad, 2006). The MAS value indicates the fraction of predicted responses from a set of random simulations, which the Absolute Relative Error is equal or less than an established threshold ($e_{MAS} = 10\%$). In this work, the metamodel is acceptable when: $\{MAS \geq 1 - e_{MAS}\}$. The relative error (e_i) compares the predicted response ($\hat{y}(i)$) with the actual CFD response ($y(i)$).

$$e_i = \frac{\left|\hat{y}(i) - y(i)\right|}{y(i)} \tag{4}$$

2.5 Performance Metrics

Performance Evaluation Criteria (PEC) for HX's is always a challenging issue. There are several metrics and methods discussed in the literature. A comprehensive discussion on the subject is beyond the scope of this paper, however, a brief introduction to the metrics selected to evaluate the HX's in this is presented. Most commonly, the evaluation is undertaken for HX's with fixed type of surfaces, i.e. the nature of the heat transfer and flow characteristics are very particular to that one surface. Because of this, the general notions on how different metrics relate to each other are better understood since they have been extensively studied and observed. The introduction of shape variables may lead to not so clear outcomes. For this reason, we use a collection of key metrics that, tentatively, will shine some light to a better understanding of the results obtained. There are two main approaches to assess the HX PEC: a) energy-based (first law of thermodynamics); b) entropy-based (second law of thermodynamics) (Zimparov & Vulchanov, 1994). The first group includes everything that quantifies the thermal-hydraulic performance and their impact on the HX geometry. The second comprehensively quantifies and qualifies all factors that affect the HX thermal-hydraulic performance (Shah, 2006).

In this work, we use the total fluid pumping power (equation 5) as a direct measure of the energy cost to deliver the desired job. The Entropy Generation Index (Ogiso, 2003) is used here in the form of a performance-degradation number (equation 6). This metric should show how the entropy generation varies with the different surfaces and how it affects the overall performance. From a geometric viewpoint, we use volume, face area and surface hydraulic diameter (equation 7) to evaluate size and compactness.

$$P_f = \dot{V}_{air} \cdot \Delta P_{air} + \dot{V}_{water} \cdot \Delta P_{water} \tag{5}$$

$$\psi_{air} = \frac{NTU}{N_s} = \frac{UA / C_{\min}}{\dot{S}_{gen,air} / C_{\min}} = \frac{UA}{\dot{S}_{gen,air}} \tag{6}$$

$$D_h = 4\frac{A_c}{A_o}d = 4\sigma\frac{V_{HX}}{A_o} \tag{7}$$

Table 1: Multi-Objective Optimization Problem.

Type	Metric	Unit	Optimization
Objectives	P_f	W	Minimize
	V_{HX}	cm³	Minimize
Constraints	Q	kW	≥ 1.0
	ΔP_{air}	Pa	$\leq \Delta P_{air\_baseline}$
	ΔP_{water}	kPa	$\leq \Delta P_{water\_baseline}$
	V_{HX}	cm³	$\leq V_{HX\_baseline}$
	r_a	-	[0.5, 1.0]
	u	m/s	[2.85, 3.0]
Parameters	V_{air}	m³/s	$V_{air\_baseline} = 0.03$
	m_{water}	g/s	$m_{water\_baseline} = 25$
MOGA Settings	Population	-	150
	Replacement	%	15
	Iterations	-	500

2.6 Multi-Objective Optimization

Studies on HX optimization have now become very common, particularly since computational power is increasing at great strides along with improved CFD codes and optimization methods like Multi-Objective Genetic Algorithms (MOGA) (method used in this paper). This work presents the application of the multi-scale analysis with topology and shape optimization method (Bacellar et al., 2016). An in-house code (Jiang et al., 2006) that allows modeling and simulation of various types of air-to-refrigerant HX's using a segmented ε-NTU approach is used for the present analysis. This tool, assisted by the metamodels, allows the optimizer to build and evaluate full sized HX designs with the novel tube shapes. The optimization problem is described in Table 1.

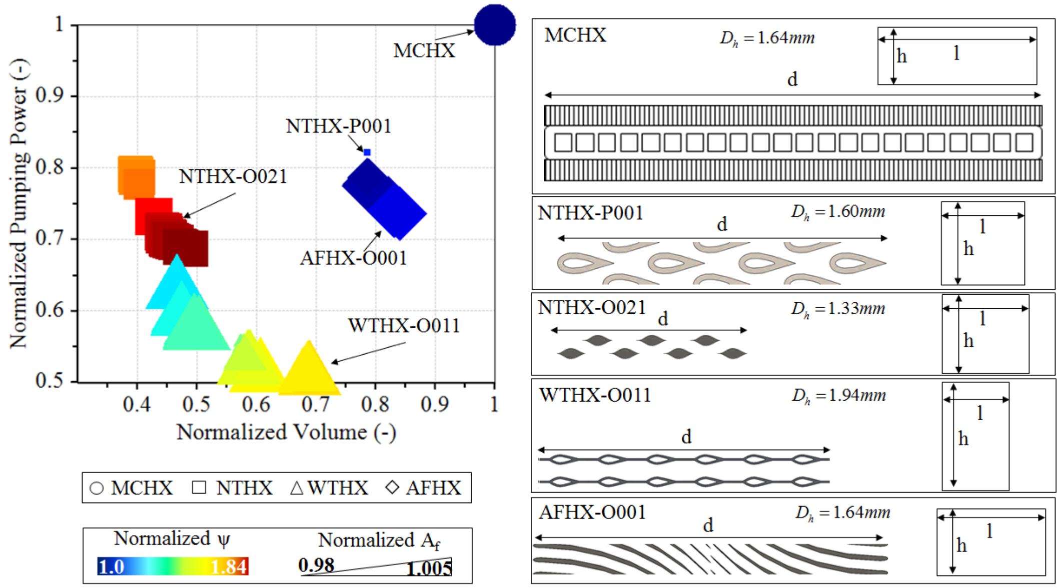

Figure 7: Optimization results.

Additive manufacturing is currently the only option for building HX's such as these. The results obtained are not yet in conformity to the additive manufacturing tolerances and accuracy. Additional runs and redesigning, using the insights from the optimum designs, lead to a viable option for prototyping, resulting in a proof-of-concept for the NTHX surface. Figure 7 maps all designs including the baseline MCHX and the prototype NTHX-P001 in a P_f vs. V_{HX} plot.

3. EXPERIMENTAL VALIDATION

The prototype of the NTHX-P001 model was tested for airside validation purposes (Huang, et al., 2016). The test facility and experiments were in accordance to the ASHRAE standards (33, 41.1, 41.2, 41.3, 41.6). The test matrix included five airflow rates and three water flow rates, resulting 15 data points, with constant 25K inlet approach temperature. The results exhibited a successful prediction of the heat transfer rate with maximum deviation of 5%, and 10% deviation for airside pressure drop.

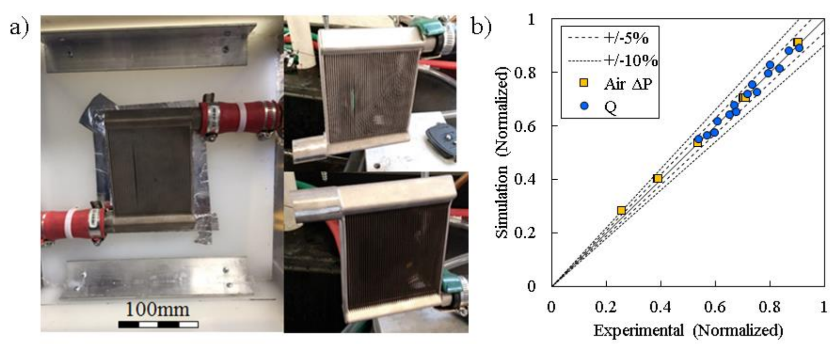

Figure 8: NTHX-001 Prototype: a) Experimental setup; b) Validation results.

4. DISCUSSION

In this section, we present a brief analysis to illustrate the mechanisms of the airflow past these surfaces on a qualitative basis. One way to do that is by plotting the contours of the velocity angle (angle of the velocity vector with respect to the x-axis). On Figure 9 it is possible to clearly identify the location, size and intensity of the air impinging the surfaces and the boundary layer detachment causing a wake region behind. The great advantage of these optimized tube shapes over conventional ones, in particular round and oval, is the reduction of the wake region and a less intense counter pressure at the impinging point. The latter is actually beneficial in terms of heat transfer, since the development of the boundary layer is undertaken at high acceleration. That is why round tubes exhibit high heat transfer coefficients, but at a cost of high hydraulic resistance.

The optimum shapes leverage the boundary layer detachment-reattachment mechanism in a more balanced way yielding overall better thermal-hydraulic characteristics. The resulting designs are remarkably interesting. While reducing size, and maintaining face area, it was possible to obtain designs with less pumping power and lower entropy generation, and yet delivering the similar capacity.

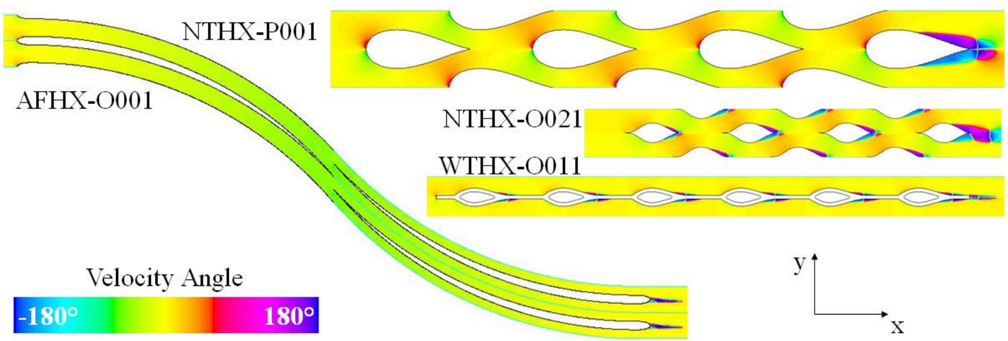

Figure 9: Velocity angle contours.

5. CONCLUSIONS

This paper presented an application of a multi-scale analysis with topology and shape optimization to a full-scale HX design. The methodology is comprehensively described, including numerical uncertainty analysis on the CFD models and metamodel prediction. Finally, we present the experimental validation of a novel heat exchanger prototype. The optimum designs suggest a potential reduction of more than 50% in size, with similar reduction in pumping power compared to the baseline MCHX. Furthermore, these designs have little to no extended surfaces, i.e. the desired thermal resistance is obtained by increasing heat transfer coefficient without the need for secondary heat transfer surfaces. Although most of these designs are still theoretical, they may not be so in near future given the rapid advancements in manufacturing technologies. The results indicate potential paradigm shift in near future with respect to HX design, optimization and manufacturing.

NOMENCLATURE

A_c	Minimum free flow area	m²	r	Grid refinement ratio	-
A_{fr}	Frontal face area	m²	ra	Aspect ratio (height / length)	-
A_o	Surface area	W/K	Re	Reynolds Number	-
C	Heat capacitance rate	J/kg.K	sgen	Entropy generation rate	W/K
c_p	Specific heat	mm	T	Temperature	K
d	Depth	m	u	Velocity	m/s
D_h	Surface hydraulic diameter	-	UA	Thermal conductance	W/K
e	Absolute relative difference	-	V	Volume	m³
F_s	Grid factor of safety		V	Volume flow rate	m³/s
GCI	Grid Convergence Index	-	ΔP	Pressure drop	Pa
h	Heat transfer coefficient	W/m².K			
h	Height	m	*Greek Letters*		
l	Tube length	mm			
NTU	Number of Transfer Units	-	δ_t	Tube thickness	mm
p	Order of accuracy	-	ε	Effectiveness	-
P	Pressure	Pa	σ	Contraction ratio (u/u_{max})	-
Q	Heat transfer rate	W	ψ	Performance-degradation number	-

ACKNOWLEDGMENT

This work was supported by the United States Department of Energy Grant Number DE-EE0006114 and the Modeling and Optimization Consortium at the University of Maryland.

REFERENCES

Abdelaziz, O., Aute, V., Azarm, S., & Radermacher, R. (2010). Approximation-Assisted Optimization for novel compact heat exchangers. *HVAC&R Research, 16*(5), 707-728.

ASHARE. (2013). *ANSI/ASHRAE Standard 41.1-2013, Standard Method for Temperature Measurement.* ASHARE.

ASHRAE. (1987). *ANSI/ASHRAE Standard 41.2-1987, Standard Methods for Laboratory Airflow Measurement.* ASHRAE.

ASHRAE. (1987). *ANSI/ASHRAE Standard 41.3-1987, Standard Method for pressure Measurement.* ASHRAE.

ASHRAE. (1987). *ANSI/ASHRAE Standard 41.6-1987, Method for Measurement of Moist Air PropertiesANSI/ASHRAE Standard 41.6-1987, Method for Measurement of Moist Air Properties.* ASHARE.

ASHRAE. (2000). *ANSI/ASHRAE Standard 33-2000, Method of Testing Forced Circulation Air Cooling and Air Heating Coil.* ASHRAE.

ASME. (2009). *Standard for verification and validation in Computational Fluid Dynamics and heat transfer - ASME V&V 20-2009.* New York: ASME.

Bacellar, D., Abdelaziz, O., Aute, V., & Radermacher, R. (2015). Novel heat exchanger design using Computational Fluid Dynamics and Approximation Assisted Optimization. *ASHRAE Winter Conference* (pp. 1-8). Chicago: ASHRAE.

Bacellar, D., Aute, V., Abdelaziz, O., & Radermacher, R. (2014). Design of Novel Air-to-Refrigerant Heat Exchangers Using Approximation Assisted Optimization. *ASME 2014 Verification & Validation Symposium.* Las Vegas, NV.

Bacellar, D., Aute, V., Huang, Z., & Radermacher, R. (2016). Muliti-Scale Analysis and Shape Optimization Method for Compact Air-To-Refrigerant Heat Exchangers. *(Submitted to the International Journal of Heat and Mass Transfer)*.

Bacellar, D., Ling, J., Abdelaziz, O., Aute, V., & Radermacher, R. (2014). Multi-scale modeling and Approximation Assisted Optimization of bare tube heat exchangers. *Multi-scale modeling and approximation assisted optimization of bare tube heat exchangers, Proceedings of the 15th International Heat Transfer Conference, IHTC-15* (pp. 1-15). Kyoto, Japan: IHTC.

DeJong, N., & Jacobi, A. (2003). Localized flow and heat transfer interactions in louvered-fin arrays. *International Journal of Heat and Mass Transfer, 46*, 443-455.

Gholami, A., Wahid, M. A., & Mohammed, H. A. (2014). Heat transfer enhancement and pressure drop for fin-and-tube compact heat exchangers with wavy rectangular winglet-type vortex generators. *International Communications in Heat and Mass Transfer, 54*, 132–140.

Hamad, H. (2006). A new metric for measuring metamodels quality-to-fit for deterministic simulations. *Proceedings of the 2006 Winter Simulation Conference.*

Hilbert, R., Janiga, G., Baron, R., & Thevenin, D. (2006). Multi-objective shape optimization of a heat exchanger using parallel genetic algorithms. *International Journal of Heat and Mass Transfer, 49*, 2567–2577.

Huang, Z., Bacellar, D., Muehlbauer, J., Ling, J., Aute, V., & Hwang, Y. (2016). Air-side performance of a novel air-to-refrigerant heat exchanger. *(Submitted to the Journal of Experimental Thermal and Fluid Sciences)*.

Jiang, H., Aute, V., & Radermacher, R. (2006). CoilDesigner: A general purpose simulation and design tool for air-to-refrigerant heat exchangers. *International Journal of Heat and Mass Transfer, 29*, 601-610.

Joardar, A., & Jacobi, A. (2005). Impact of leading edge delta-wing vortex generators on the thermal performance of a flat tube, louvered-fin compact heat exchanger. *International Journal of Heat and Mass Transfer, 48*, 1480–1493.

Kasagi, N., Suzuki, Y., Shikazono, N., & Oku, T. (2003). Optimal design and assessment of high performance micro bare-tube heat exchangers. *Proc. 4th Int. Conf. on Compact Heat Exchangers and Enhancement Technologies for the Process Industries.* Crete, Greece.

Kays, W., & London, A. (1984). *Compact heat exchangers* (3rd ed.). New York: McGraw-Hill.

Koplow, J. (2010). *A Fundamentally New Approach to Air-cooled Heat Exchangers.* Albuquerque, New Mexico 87185 and Livermore, California 94550: Sandia National Laboratories.

Matos, R., Laursen, T., Vargas, J., & Bejan, A. (2004). Three-dimensional optimization of staggered finned circular and elliptic tubes in forced convection. *International Journal of Thermal Sciences*, 477-487.

Min, J., & Webb, R. (2004). Numerical analyses of effects of tube shape on performance of a finned tube heat exchanger. *Journal of Enhanced Heat Transfer, 11*(1), 61-73.

Ogiso, K. (2003). Duality of heat exchanger performance in balanced counterflow systems. *Journal of Heat Transfer, 125*(3), 530-532.

Paitoonsurikarn, S., Kasagi, N., & Suzuki, Y. (2000). Optimal design of micro bare-tube heat exchanger. In P. Cheng (Ed.), *Proceedings of Symposium on Energy Engineering in the 21st Century, 3*, pp. 972-979. Hong Kong.

Ranut, P., Janiga, G., Nobile, E., & Thevenin, D. (2014). Multi-objective shape optimization of a tube bundle in cross-flow. *International Journal of Heat and Mass Transfer, 68*, 585-598.

Roach, P. (1997). Quantification of Uncertainty in Computational Fluid Dynamics. *Annual Review of Fluid Mechanics, 29*, 123–160.

Roy, C., & Oberkampf, W. (2011). A comprehensive framework for verification, validation, and uncertainty quantification in scientific computing. *Computational Methods Applied to Mechanical Engineering, 200*, 2131–2144.

Shah, R. (2006). Advances in science and technology of compact heat exchangers. *Heat Transfer Engineering, 27*(5), 3-22.

Shah, R., & Sekulic, D. (2003). *Fundamentals of Heat Exchanger Design* (2nd ed.). New Jersey: John Wiley & Sons.

Webb, R., & Kim, N. (2005). *Principles of enhanced heat transfer.* New York: Taylor&Francis.

Zimparov, V., & Vulchanov, N. (1994). Performance evaluation criteria for enhanced heat transfer surfaces. *International Journal of Heat and Mass Transfer, 37*(12), 1807-1816.